7-1-1991

Modeling Ultrasound Speckle Formation and its Dependence on Imaging System's Impulse Response

Navalgund A. H. K. Rao
Rochester Institute of Technology

Hui Zhu
Rochester Institute of Technology

Recommended Citation
Navalgund A. H. K. Rao, Hui Zhu, "Modeling ultrasound speckle formation and its dependence on imaging system's response", Proc. SPIE 1443, Medical Imaging V: Image Physics, (1 July 1991); doi: 10.1117/12.43432; https://doi.org/10.1117/12.43432

Transfer copyright and understand use restrictions

Transfer Copyright

Once your paper is accepted for publication, you may return the Transfer of Copyright form by any of the following methods: (1) scan the signed form and return it as an e-mail attachment to journals@spie.org, (2) fax it to 1-360-647-1445, or (3) mail it to SPIE Journals Dept., PO Box 10, Bellingham, WA 98227-0010 USA.

Use Restrictions

Posting papers on personal websites: Authors, or their employers in the case of works made for hire, retain the right to post a preprint or reprint of their paper on an internal or external server controlled exclusively by the author/employer, provided that (a) such posting is noncommercial in nature and the paper is made available to users without a fee or charge; and (b) the following statement appears on the first page, or screen, of the paper as posted on the server:

Copyright 1991 Society of Photo-Optical Instrumentation Engineers.

This paper was (will be) published in Medical Imaging and is made available as an electronic reprint (preprint) with permission of SPIE. One print or electronic copy may be made for personal use only. Systematic or multiple reproduction, distribution to multiple locations via electronic or other means, duplication of any material in this paper for a fee or for commercial purposes, or modification of the content of the paper are prohibited.

Obtaining permission to use previously published material from an SPIE journal: Please send an e-mail to reprint_permission@spie.org and include the following information in your request: title and author, volume and page numbers, what you would like to reproduce, and where you will republish the requested material. Requests may also be faxed to SPIE at 1-360-647-1445 (Attention: Permissions).

Copying a paper from the journal: Copying of material in SPIE journals for internal or personal use, or the internal or personal use of specific clients, beyond the fair use provisions granted by the U.S. Copyright Law is authorized by SPIE subject to payment of copying fees. The Transactional Reporting Service base fee for SPIE journals is $25.00 per article (or portion thereof), which should be paid directly to the Copyright Clearance Center (CCC), 222 Rosewood Drive, Danvers, MA 01923. Other copying for republication, resale, advertising or promotion, or any form of systematic or multiple reproduction of any material in an SPIE journal is prohibited except with permission in writing from the publisher. The CCC fee code (which consists of ISSN/year/fee, e.g., 0091-3286/07/$25.00) is published at the bottom of the first page of each journal article.

MODELING ULTRASOUND SPECKLE FORMATION AND ITS DEPENDENCE ON IMAGING SYSTEM'S REPONSE

Navalgund Rao and Hui Zhu
Center for Imaging Science
Rochester Institute of Technology
Rochester, NY 14623

ABSTRACT

Ultrasonic echoes, backscattered from an inhomogeneous medium have the character of a random signal, which is mainly responsible for the observed speckle in medical images. Such a medium can be modeled as a uniform matrix with scattering bodies distributed randomly. When the number of density of scatterers is high, the individual scatterers are not resolved by the imaging process, and a speckle pattern is produced as a result of interference of waves from many scatterers within the resolution cell volume. This cell volume depends on the beam profile and the pulse width of the interrogating pulse. We have used a 3 dimensional (3D) simulation phantom that takes into account the 3D distribution of scatterers and the 3D nature of the resolution cell volume. Several simulations were performed to study the effect of scatterer number density (SND) and resolution cell volume on the backscattered signal. Assuming the process is linear and the stochastic signal is ergodic and stationary, Kurtosis (K), which involves 2nd and 4th moments, was estimated in each case. We find that Kurtosis varies linearly with another parameter F_s that depends on the resolution cell volume. The results are analyzed in the light of theoretical predictions. Reasonable estimates of SND can be derived from the slope of Kurtosis vs. parameter F_s graph.

1. INTRODUCTION

Speckle patterns in imaging systems such as ultrasound B-scans are classically interpreted as the result of coherent summation of responses from a large number of scattering targets. The central limit theorem can then be invoked: The RF signal amplitude exhibits a Gaussian distribution from which a Rayleigh distribution is deduced for signal envelope and an exponential distribution for signal intensity [1]. The signal-to-noise ratio (SNR), defined as the ratio of the mean to standard deviation of the distribution, then reaches a limiting value of 1.91 for signal envelope and 1.0 for signal intensity. In this, so called Rayleigh limit case, parameters derived from the first order statistics of the signal, such as SNR, become independent of the imaging system parameters and the scatterer density. However, if the mean distance between scatterers is not negligible with respect to the resolution-cell size of the imaging system, the scatterer density cannot be considered "very large" any more. The speckle statistics will depend on the scatterer distribution and the resolution cell size of the system. Based on this behavior, it has been suggested that parameters derived from speckle statistics may be useful for tissue characterization, provided we are below the Rayleigh limit [2]. This limit can be reached, either by changing scatterer number density or the resolution cell volume. In a tissue characterization problem, the former is not under our control, but the later depends on the imaging system and hence could be adjusted.

Although the influence of resolution cell size has been appreciated before, it's usefulness has not been evaluated. This paper examines this question through theoretical simulation. In section 2

we develop a 3-dimensional comprehensive model of the random tissue structure characterized by a mean scatterer spacing. A procedure that uses frequency modulated (FM) pulse for imaging is outlined. The advantage of the FM pulse over the conventional short pulse is that the resolution cell volume can be varied easily by changing the center frequency f_o and bandwidth Δf of the interrogating pulse. In section 3, procedure to simulate RF signal backscattered from the tissue model is outlined. Three different tissue models were examined and each model was interrogated with five different frequency modulated pulses. The simulation procedure takes into account the 3-D nature of the resolution cell volume and its effect on the RF signal. In section 4, we examine the data analysis of RF signal for tissue characterization. The signal is considered as a stochastic random variable. Statistical moments of the signal are calculated as useful feature parameters characterizing the tissue model. However, these moments are biased by the imaging systems point spread function or resolution cell volume. A theory developed for RF signals [2] is considered that shines some light on how this bias can be analyzed. A procedure is outlined to estimate "scatterer number density" characterizing the tissue model.

2. THEORETICAL SIMULATION

2.1. Frequency Modulated Pulse for Imaging

We have been investigating the possibility of soft tissue imaging using frequency modulated (FM) pulses [4,5]. Instead of a conventional short pulse, a linearly swept frequency modulated, longer duration interrogating pulse is used. By a process of cross-correlation, this longer duration FM pulse can be compressed into a short pulse. Assuming that the generation of backscattered signal is a linear process, the concepts and tools of linear systems theory can be used as shown in figure 1. The real usefulness of this technique in medical imaging comes from the fact that the process of pulse compression can be carried out after the backscattered signal has been received. Figure 1 below shows where the post processing step is incorporated [3].

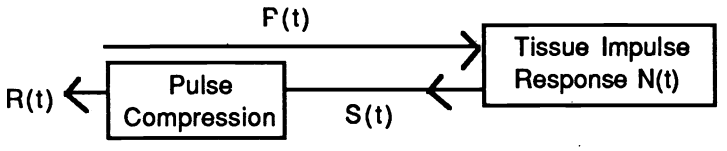

Figure 1

P(t) is the input FM pulse and N(t) represents the tissue impulse response. For a non attenuating medium, N(t) is simply a sum of delta functions, $\sum_i \omega_i \delta(t-ti)$ where ω_i is the reflection coefficient of the i th scatterer, located at a distance $z_i = c.ti/2$, c being the speed of sound and ti is two way travel time. Treating the pulse propagation and reflection as a linear process, the backscattered signal S(t) can be expressed as a convolution of P(t) with N(t):

$$S(t) = P(t) * N(t) \qquad (1)$$

$$R(t) = P(t) \bullet S(t) = P(t) \bullet P(t) * N(t) = A(t) * N(t) \qquad (2)$$

The process of pulse compression is carried out by cross-correlating the input FM pulse P(t) with the received backscattered signal S(t), denoted by (•), as shown in equation (2). The autocorrelation of P(t) results is a compressed short pulse A(t), whose peak amplitude is greater than that peak amplitude of the FM pulse by a factor K. This gain factor K is equal to the product of the time duration and the effective bandwidth of the FM pulse. The pulse width of the compressed pulse only depends on the bandwidth of the FM pulse.

2.2. The Three Dimensional Point Spread Function

The process described above would produce a single A-line signal which is one dimensional in nature. Time t encodes the depth coordinate z. By moving the transducer axis to an adjacent location, and displaying all A-lines together, one generates a two-dimensional image. Although the A-line signal represents a one-dimensional image of the object, it should not be forgotten that physical phenomena take place in the "real space," known to be three-dimensional. The tissue and their echo-generating structures have a spacial extent and no transducer can exactly focus the ultrasound beam on a line or a plane. This is why the impulse response characterizing an echo graphic system should have a 3D spacial dependence on the target position. The 3D point spread function (PSF) is defined as follows: any point in space is referenced in a cartesian system of coordinates (Ox, Oy, Oz); a transducer can be moved in a plan (Ox, Oy) while keeping its axis parallel to the Oz axis which is also colinear with the transducer beam axis; a target location is determined by coordinates (x_o, y_o, x_o). The contribution of this target to the 3-D image is the value of the target response at time $2z_{o/c}$ when the transducer is located at (X, Y, Z, = 0).

For a circularly symmetric transducer, the backscattered RF signal from a target at (x_o, y_o, z_o,) can be written as

$$S(r,\ z_o,\ t) = \omega \cdot P(t) * B(r,\ t,\ z_o)\ ;\ t = 2z_{o/c} \qquad (3)$$

where r is the radial distance of target from the central axis of the beam.

$\left[r = \sqrt{(X - x_o)^2 + (Y - y_o)^2 + z_o^2} \right]$, P(t) is the FM pulse response at r = o, and ω is a constant that depends on scattering strength. $B(r,t,z_o)$ describes the beam shape of the system at depth z_o. The convolution is with respect to time t. The PSF of the FM pulse imaging scheme is determined after pulse compression processing i.e. after cross correlation of $S(r, z_o,t)$ with P(t);

$$PSF(r,\ z_o,t) = \omega \cdot P(t) \bullet P(t) * B(r,t,z_o) \approx \omega \cdot h(t) * \delta(t - 2z_{o/c}) \cdot B(r,\ z_o) \qquad (4)$$

The pulse width of the compressed pulse {P(t) • P(t)} mainly determines the resolution in the axial direction. In the FM pulse imaging scheme this can be controlled by the frequency bandwidth Δf of the FM pulse. The lateral resolution is controlled by the beam response $B(r,t,z_o)$. For a narrow bandwidth excitation $B(r,t,z_o)$ can be approximated as $\delta(t - 2z_{o/c}) \bullet B(r,z_o)$ where $B(r,z_o)$ is given by the classical far field diffraction pattern due to circular aperture. Therefore, to 1st order $B(r,t,z_o)$ depends on the center frequency of excitation, f_o. Without this approximation, one would have to consider exact impulse response of transducer. Use of FM pulse in the simulation has been considered because of the ease with

which both f_o and Δf can be changed. By changing f_o and Δf, it is possible to bring about change in the PSF in the lateral and axial direction. Equation (4), after approximation, states that the contribution to the RF signal from a scatterer located at (r, z_o) is simply the time delayed compressed pulse, scaled by the scattering strength (ω) and the beam response value, B(r, z_o).

z_o is assumed to be at the center of the focal zone of the transducer. In the focal plane of a spherically focused transducer, the beam shape B(r, z_o) can be approximated by the well known airy pattern [6]

$$B(r,z_o) = (\text{constant}) \cdot \left[\frac{2J_1(x)}{x}\right]^2 \quad \text{where } x = \left(\frac{2\pi f_o \cdot d \cdot r}{c \cdot z_o}\right) \qquad (5)$$

2d is the transducer diameter and z_o is the focal length. The square of the airy pattern is used here because the PSF defined in (4) involves backscattering i.e. illumination and reception of signal from a scatterer located in the beam.

2.3. Theoretical Simulation of RF Signal

For a fixed location of the transducer, the backscattered RF signal received from a region in the focal zone, can be different for different input interrogating pulses. This is so, because different input pulses will have different 3D point spread function (or resolution cell volume) as shown in figure 2. The simulation procedure we have used is particularly useful for studying changes in the RF signal as a function of beam width (BW) and/or pulse width (P). The procedure is based on a computer model described by Kuc et.al. [7]. It was modified to incorporate changes in the 3D point spread function as a function of f_o and Δf of the interrogating FM pulse. The simulation model is composed of a transducer model and that of the random scattering medium. The former provides a description of the ultrasound field at a scatterer location, while the latter specifies the probability laws governing the random scattering strengths and locations.

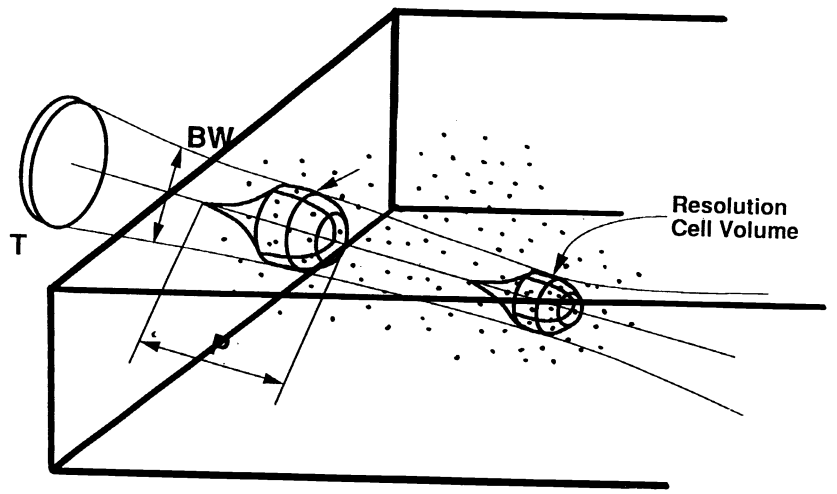

Figure 2

(a) TRANSDUCER MODEL: We consider a circular transducer that is spherically focused at a distance z_o. The 3D space of the random medium in the focal zone, interrogated by the field of view of the transducer is approximated by a cylinder as shown in figure 3. The diameter corresponds to the largest beam width (at the lowest frequency f_o). The length of the cylinder corresponds to the time duration of the A-line RF signal that is of interest. The central axis of the cylinder coincides with the transducer axis and is also collinear with z axis. The contribution to A-line RF signal from a scatterer located at (r,z_O) is simply a weighted PSF at that location, given by equation (4). The one dimensional A-line RF signal, can be computed in principle by convolution operation. The approximation in equation (4) reduces this operation to a summation of appropriately scaled responses from all the scatterers in the cylindrical volume. Because of the radial symmetry of the PSF, this 3D problem can be simplified into a set of 1D problem. The field of the transducer is partitioned into a set of cylinders or microbeams, which are parallel to the axis of the transducer, as shown in Fig. 3.

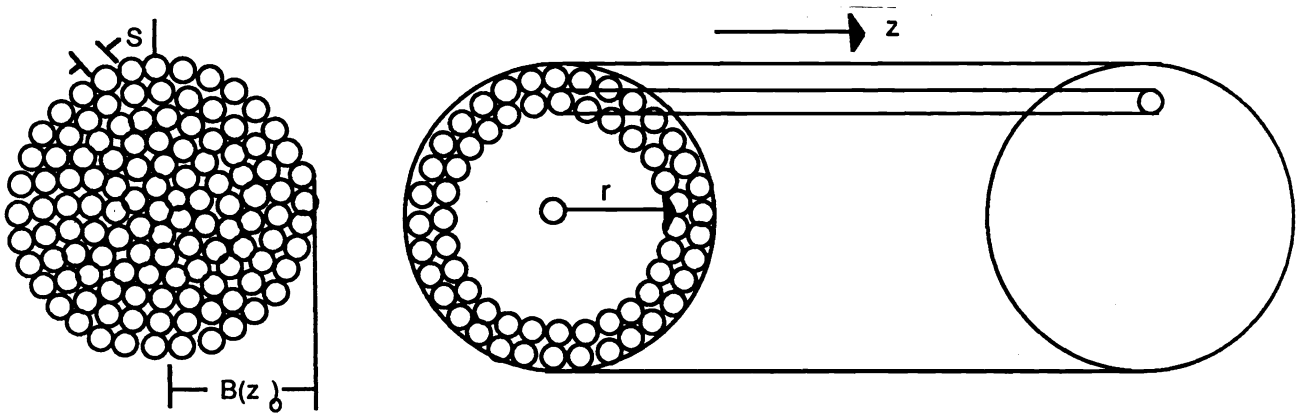

Figure 3 Division of 3D scattering into 1D microbeams

The radius of the microbeams is determined by the mean spacing of the scatterers, S. The beam cross section is divided into a set of annuli of constant thickness, equal to the mean scatterer spacing S. The center radius of annulus k is then $r_k=(k-1)S$, for $1< K < N_A$, where

$$N_A=[B(z_0)/S + 0.5] \qquad (6)$$

where the bracketed quantity denotes the value truncated to the nearest integer. A set of microbeams, each having diameter S, is then packed into each annulus. The number of microbeams in the kth annulus is

$$N_M(k)=(2\pi r_k/S)=]2\pi(k - 1)], \text{ for } 2\leq k\leq N_A \qquad (7)$$

with $N_M(1)=1$. A random reflector sequence can then be generated for each microbeam, as described below.

(b) STOCHASTIC MODEL OF RANDOM SCATTERERS: The tissue was modeled as a set of scatterers having random scattering strengths and randomly located within each microbeam. The

microbeam approximation constrains the separation between the independent spacial sequences to be approximately equal to the mean spacing S. This allows the use of one dimensional probability function to describe the random spacing in 3 dimensions.

The scattering strength ω_n was a random variable with a gaussian probability distribution of zero mean and standard deviation 0.5. Within each microbeam the distance between scatterers n-1 and n was also a random variable, with an exponential probability density function with a mean value of S. Governed by these two probabilities we generate the reflector sequence for the jth microbeam in the kth annulus, denoted by $m_{k,j}(t)$.

$$m_{k,j}(t) = \sum_{n=1}^{N_M} \omega_n \delta(t - t_n) \qquad (8)$$

Assuming that the detection process of the transducer is linear, the total reflected signal is equal to the sum of the contributions from each microbeam. Since the microbeam within a given annulus are equidistant from the central axis, their reflector sequences can first be added and then the annular sum can be convolved with the reflector impulse response of the transducer appropriate for the given annulus. The composite backscattered signal $r(t,z_0)$ is then equal to

$$r(t,z_0) = \sum_{k=1}^{N_A} \left(PSF(r_k, z_0, t) * \sum_{j=1}^{N_M} m_{k,j}(t) \right) \qquad (9)$$

Using the approximation for the PSF, $h(r, z_0,t)$, defined in equation (4) of section 2.2, we can write the backscattered signal as

$$r(t,z_0) = h(t) * \sum_{k=1}^{N_A} B(r_k, z_0) \cdot \sum_{j=1}^{N_M} m_{k,j}(t) \qquad (10)$$

3. SIMULATION OF RF SIGNAL

A spherically focused transducer of radius 2.4 cm and a focal length z_o of 5.0 cm is considered for simulation. The speed of sound c, in the medium is assumed to be 1560 meters/sec. The lowest center frequency of operation was 1 MH_z. Therefore the maximum size of the beam shape $B(z_o)$ was calculated from equation (5) as the radial distance where the $B(r, z_o)$ hits its first zero. $B(z_o)$ was found to be 2 mm and the geometry of the microbeam was set using this and the mean scatterer space S (see figure 3).

The steps taken in simulation process are outlined below. Examples for the model with mean scatterer spacing S = 0.3 mm are also given.

(1) The number of annulus N_A is calculated by using equation (6), and the number of microbeams in kth annulus N_M described by equation (7) is then computed.

(2) Statistically independent realization of the random reflector sequence for each microbeam in a given annulus is generated as described by equation 2. A set of random number, that are exponentially distributed with a mean value of S = 0.3 mm were generated, to be used as random scatterer spacing within each microbeam. The scattering strength, ω_n was also a random variable with a gaussian distribution with zero mean and a standard deviation of 0.5. Figure 4 is an example of one such microbeam discrete reflector sequence $m_{k,j}(t)$. The sampling interval was Δt = 0.05 μs. The total length of the sequence is 512 points which corresponds to 26.6 μs of two way travel time. This is equivalent to approximately 2 cm of tissue in axial direction. Each delta function indicates a location of a scatterer in the jth microbeam of the kth annulus. The amplitude of the delta function is given by the reflection strength ω_n of the scatterer. The spacing between delta functions is given by (n.Δt), which corresponds to spacial separation of $\Delta s = (c.n.\Delta t)/2$. Here n is the random variable which is exponentially distributed and has a mean such that the mean of Δs is equal to mean scatterer spacing of the model, i.e. 0.3 mm.

(3) All the microbeam discrete sequences were stored in computer memory to be used for simulating backscatter response. The interrogating FM pulse has two parameter, f_o the center frequency and Δf, the bandwidth. The following steps were taken to simulate RF signal in response to a particular FM pulse. The steps are repeated for every FM pulse characterized by f_o and Δf.

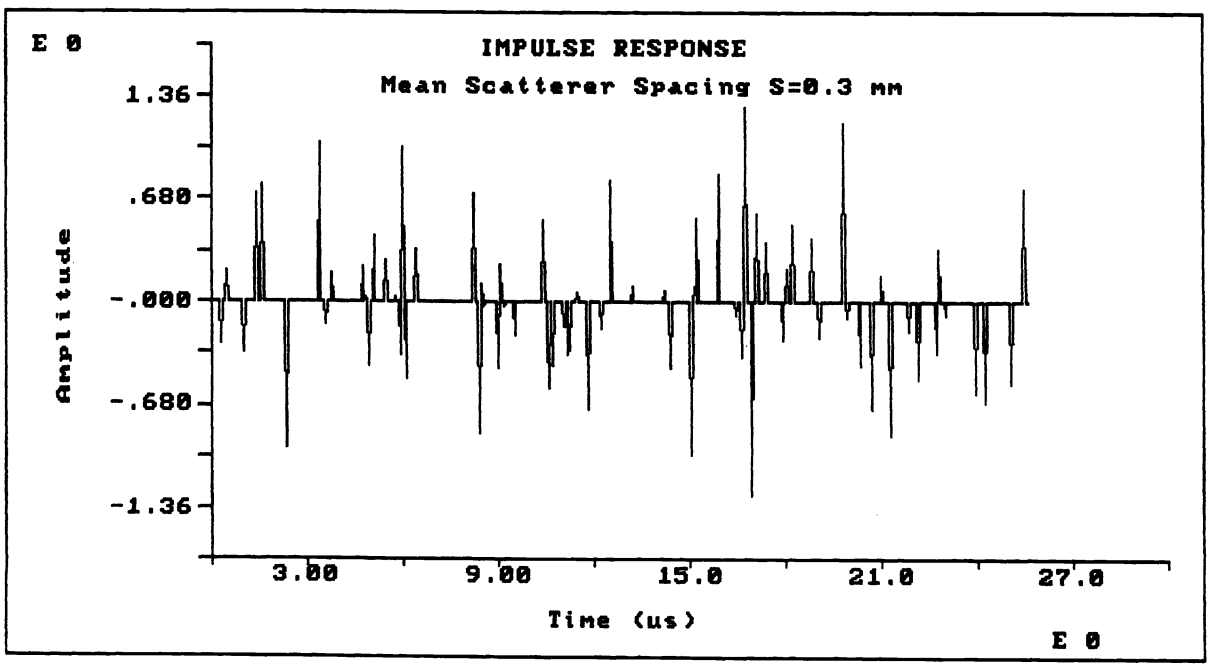

Figure 4 One realiation of 1D impulse response within a microbeam

(4) All the sequences corresponding to the same annulus k are added together and then weighted by the value of the beam pattern at the radium r_k. The beam pattern has been approximated by the directivity function $B(r,z_0)$ in equation (5) and is a function of center frequency f_o of the FM pulse. One example is shown in Figure 5, for f_o = 1 MH_z.

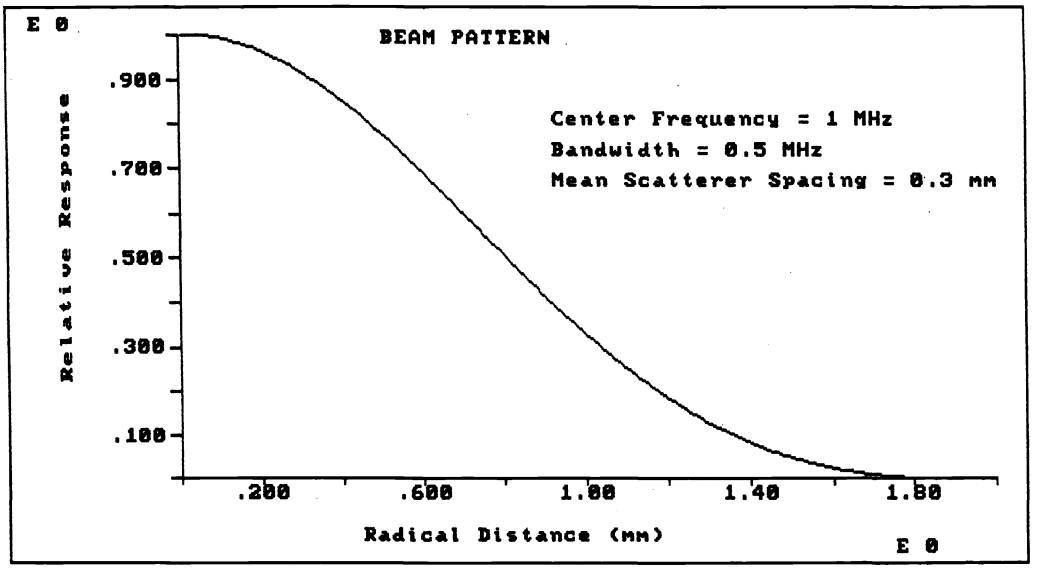

Figure 5 Circularly symmetric beam pattern of the transducer operating at 1 MH_z

(5) The contributions from all annuli are added together to form the composite reflector sequence as shown in Figure 6. This corresponds to the term on the right hand side of convolution sign in equation (10).

(6) This sequence is then convolved with a frequency modulated pulse (FM pulse) h(t) {Fig. 7} to produce the backscattered signal {Fig. 8}, which is then correlated with h(t) (pulse compression step) to produce the RF signal shown in Fig. 9. The FM pulse has the center frequency f_o = 1 MH_z, which is consistent with the beam profile calculations. In the above example, the bandwidth Δf was equal to 0.5 MH_z. These two parameters were determined from the power spectrum.

(7) Simulation of different RF signals in response to different FM pulses at the same transducer location, was carried out by repeating steps 4 through 6 for different pulse parameters. Every tissue model was probed with five different FM pulses. The parameters used are given in Table 1, along with the 6dB width of the compressed pulse and the 6dB beam width.

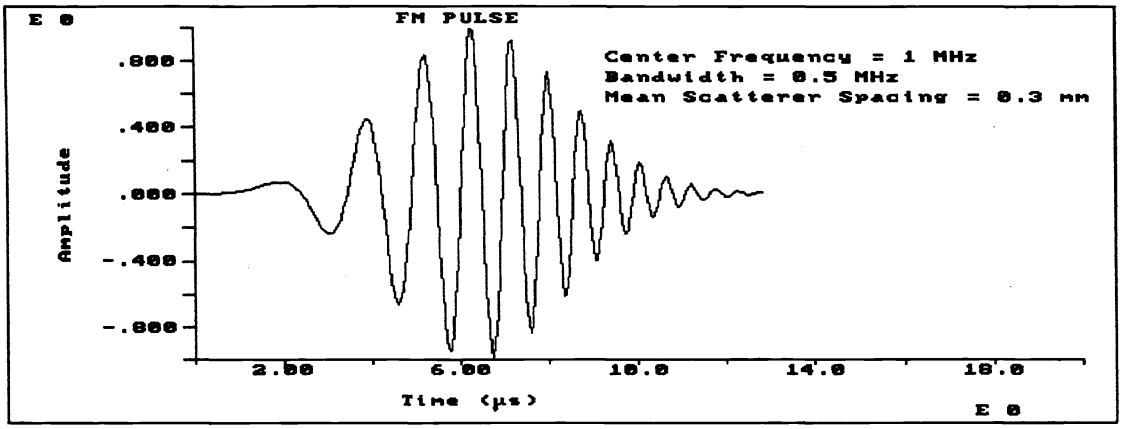

Figure 6

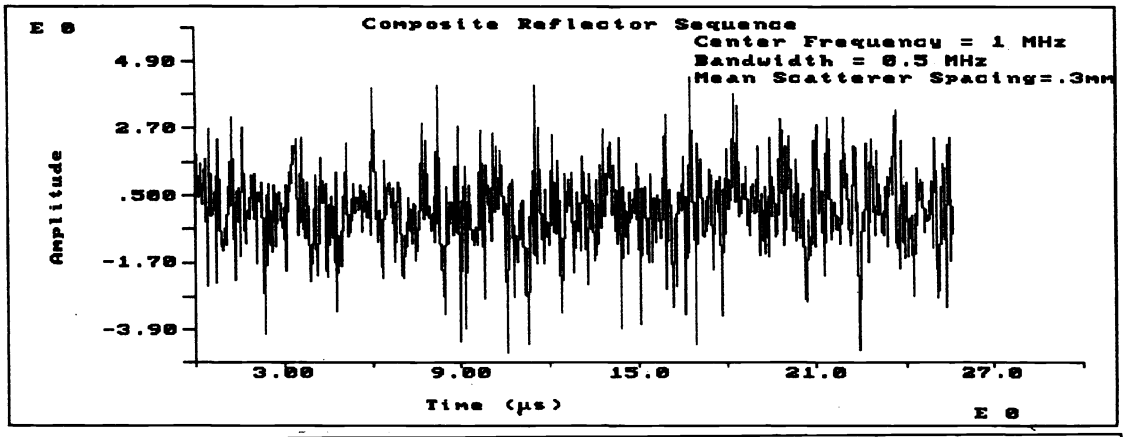

Figure 7

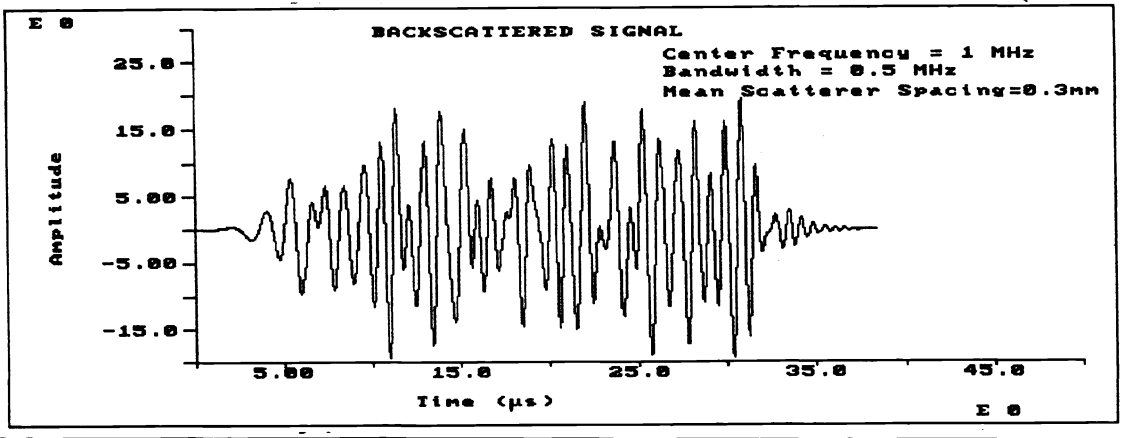

Figure 8

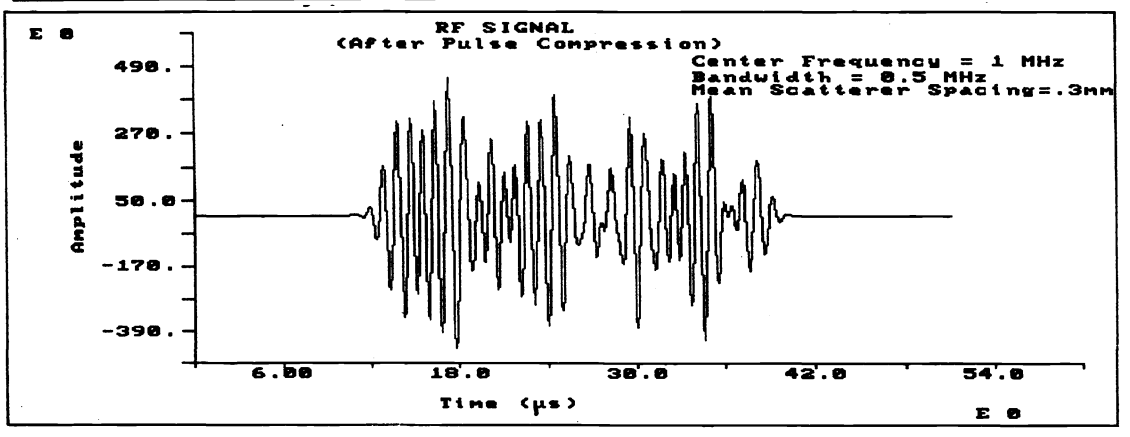

Figure 9

TABLE 1 - Imaging Pulse Parameters

Center Frequency f_o MH_z	Band Wdith Δf MH_z	Pulse Width μS	Beam Width mm	F_s $(mm)^{-3}$
1.00	0.50	1.60	1.59	0.42
2.00	1.02	0.80	0.81	3.19
3.00	1.57	0.50	0.53	10.63
2.00	0.50	1.60	0.83	1.55
3.00	1.02	0.80	0.55	6.89

4. STOCHASTIC APPROACH TO RF SIGNAL ANALYSIS

The RF signal backscattered from an inbomogeneous parenchymal tissue has the character of a random signal. We also find a similar structure in the simulated RF signal shown in Figure 10. It has been suggested that 1st and 2nd order statistics of the RF and envelope detected video signal be used for tissue characterization [9,10]. However, the statistical nature of the RF signal depends, not only on the random tissue scattering structure, but also on the resolution cell volume of the imaging system. This is exemplified by simulated RF signals shown in Figure 9. Two different RF signals are shown, both resulting from the same random tissue model (mean scatterer spacing S = 0.3 mm). The top graph is from a low resolution imaging system with f_o = 1 MH_z and Δf = 0.5 MH_z and the bottom graph is from a high resolution system with f_o = 4 MH_z and Δf = 2.I MH_z. These extreme examples were chosen to qualitatively demonstrate the differences in the random nature of the signal from the same tissue model. Quantitatively, the difference can be parameterized by Kurtosis K, which is the ratio of the 4th moment to the square of the 2nd moment. Value of 2,85 and 5.12 is obtained for the two cases. Clearly, this difference is due to the differences in the point spread function of the two systems. For the case in Figure 9, both the beam shape and the pulse width contribute to this difference, while the "imaged" mathematical phantom remains the same. For the purpose of tissue characterization, it is important to understand and separate this signature of the imaging system. The major objective of this section is twofold; (i) quantitatively analyze the role of the imaging system's point spread function (PSF), (ii) develop data analysis techniques to extract parameters that are independent of the system's PSF. The analysis is performed on the RF signal obtained through simulation described in the previous section.

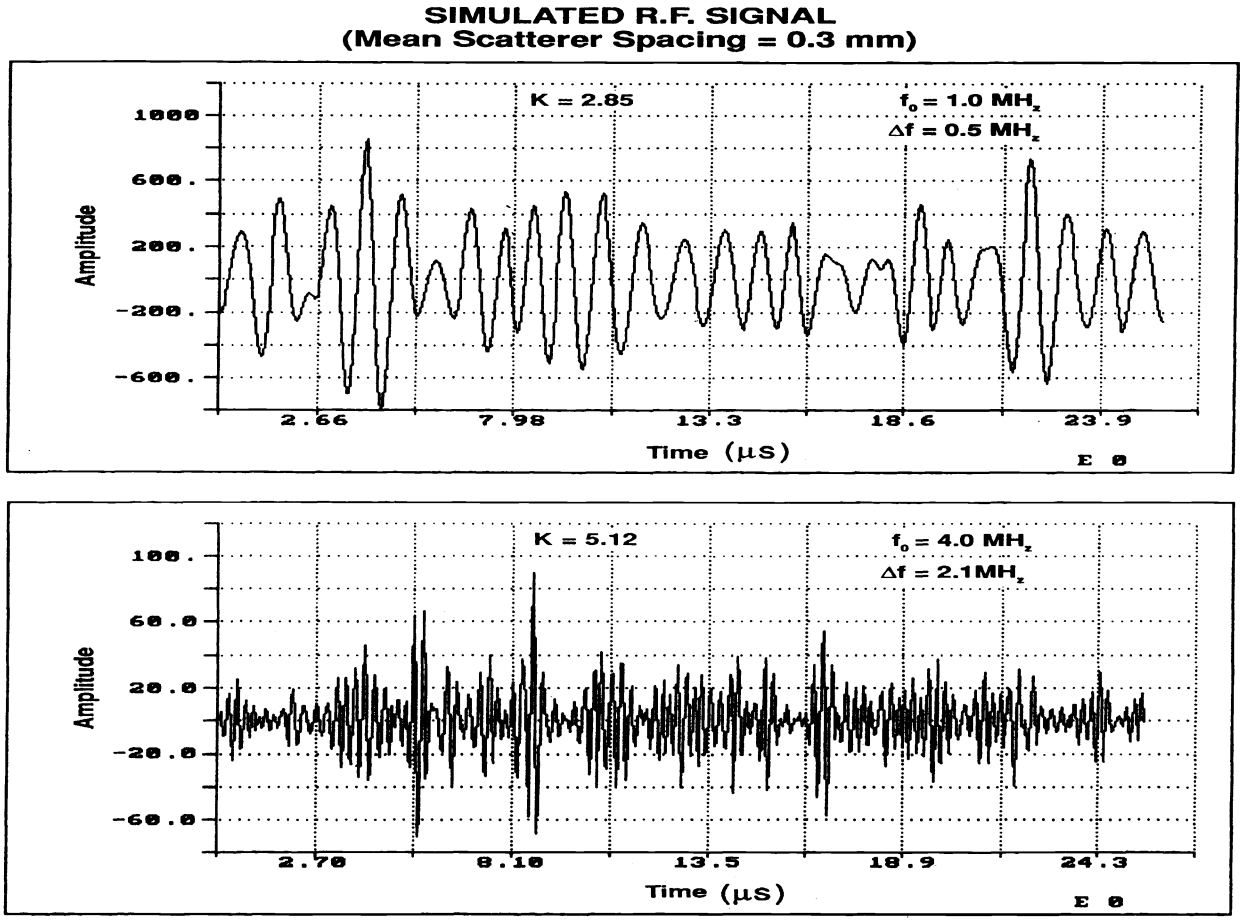

Figure 10 One realization of simulated RF signal from a model with S = 0.3 mm for two different input pulses

RF signal becomes uncorrelated if the transducer is moved in the lateral direction by a distance greater than the beam width. These uncorrelated signals represent different realization of the same stochastic process that we wish to characterize. If the field of view is small, we can assume that the process is wide-sense stationary and ergodic. The former assumption facilitates ensemble averaging while the latter, time averaging, in the estimation of statistical moments. Therefore, we have simulated 20 statistically independent RF signals for every pulse parameter and every tissue model under study. Every statistical moment calculated is a result of ensemble and time averaging over 20 RF signals.

4.1. Departure from Gaussian Statistics

The random character of the backscattered RF signal results from the phase-sensitive detection of the scatter from many sites randomly distributed in the resolution cell of the transducer, together with the scanning of this cell through the medium. The resolution cell volume can be roughly defined as the "effective" space occupied by the PSF [11]. The process of interference can be described geometrically as a random walk of component phasors. When the number of scatterers N within one resolution cell is large, and the phases of the scattered waves are

independent and distributed uniformly between 0 and 2π, the phasor or complex field amplitude a, which is the result of the random walk, has real and imaginary components a_r and a_i whose joint probability density function (pdf) is circularly gaussian [12]. The RF signal is considered as the real part of this complex field. In the limit of large number of scatterers within a resolution volume, the backscattered RF signal has a zero mean gaussian pdf and therefore has an expectation value of 3 for Kurtosis [9]. This limit is reached in our simulation for the case shown by the top RF signal in Figure 10 The resolution cell volume there is large enough to satisfy the large N condition. The value of Kurtosis is 2.75 and not exactly 3 because it is obtained from one single realization of the random process and no ensemble averaging has been carried out. The bottom RF signal of figure 9 is a case in point where significant departure from the gaussian pdf has taken place because the resolution cell volume is smaller and the number of scatterers within the cell can no longer be considered "large." Note that the interrogated random medium is the same in both cases, characterized by mean scatterer spacing S=0.3 mm. It is this departure from gaussian statistics, as evidenced by the deviation from 3, in the value of Kurtosis, that we wish to investigate.

Sleefe and Lele have considered a stochastic model for the backscattered signal. The random medium is approximated as a homogeneous matrix material with scattering bodies randomly distributed throughout in 3 dimensions. The medium is described by two random variables. The location of a scatterer in a given volume is uniformly distributed with number of scatterers in the volume obeying Poisson probability law. An average value for number of scatterers per unit volume or SND (scatterer number density) defines the random scatterer spacing in the medium. The scattering strength ω is another random variable with an expectation value $E[\omega]$. The backscattered RF signal r(t), is also considered a random variable, with an expectation value E[r]. They also consider a 3D point spread function defined as a product of the 2D beam pattern B(x,y) = B(r) and the pulse shape h(t). An expression was derived relating all the parameters considered above:

$$K - 3 = \left[\frac{F_m}{SND}\right] \cdot F_s \qquad (11)$$

where

$$\text{Kurtosis } K = E[r^4(t)]/E^2[r^2(t)] \qquad (12)$$

$$F_m = E[\omega^4]/E^2[\omega^2] \qquad (13)$$

$$F_s = \frac{2\int_{-\infty}^{+\infty} B^4(r).h^4(t).2\pi r.dr.dt}{C\left\{\int_{-\infty}^{+\infty} B^2(r).h^2(t).2\pi r.dr\,dt\right\}^2} \qquad (14)$$

E[r(t)] and $E[\omega]$ refer to statistical 1st moments of the RF signal and the random scattering strengths respectively. Kurtosis in equation (12) is defined as the ratio of the 4th moment to the square of the 2nd moment of the RF signal. F_m is a parameter similar to Kurtosis, calculated

on the random variable ω. B(r) is the circularly symmetric beam pattern and h(t) is the autocorrelation of the FM pulse. F_s is a parameter that depends on the point spread function of the imaging system. It is inversely proportional to the resolution cell volume.

4.2. Analysis of the RF Signal

Equation (11) describes the departure of the RF signal from gaussian behavior. The random medium is characterized by two parameters, F_m and SND. F_s carries information about the imaging systems point spread function. Kurtosis K characterizes the stochastic nature of the RF signal. We have analyzed our simulated RF data in the light of this theory. Kurtosis is calculated by performing discrete sum of powers of RF signal i.e

$$K = \frac{1}{(512)} \sum_{i=1}^{512} r^4 (i\,\Delta t) \,/\, [r^2 (i\Delta t)]^2 \qquad (15)$$

An ensemble average is also performed over all the 20 independent RF A-line data for each case. The parameter F_s is calculated numerically by evaluating the integrals in (14). Both B(r) and h(t) are completely determined by fo, Δf and the transducer parameters. Table 1 lists the calculated values of F_s for all the 5 cases. Scatterer number density (SND) can be identified with $(1/S^3)$ where S is the mean scatterer spacing in our models. The scattering strengths of discrete scatters are zero mean gaussian distributed. Therefore, the parameter F_m has a value of 3 for our simulations.

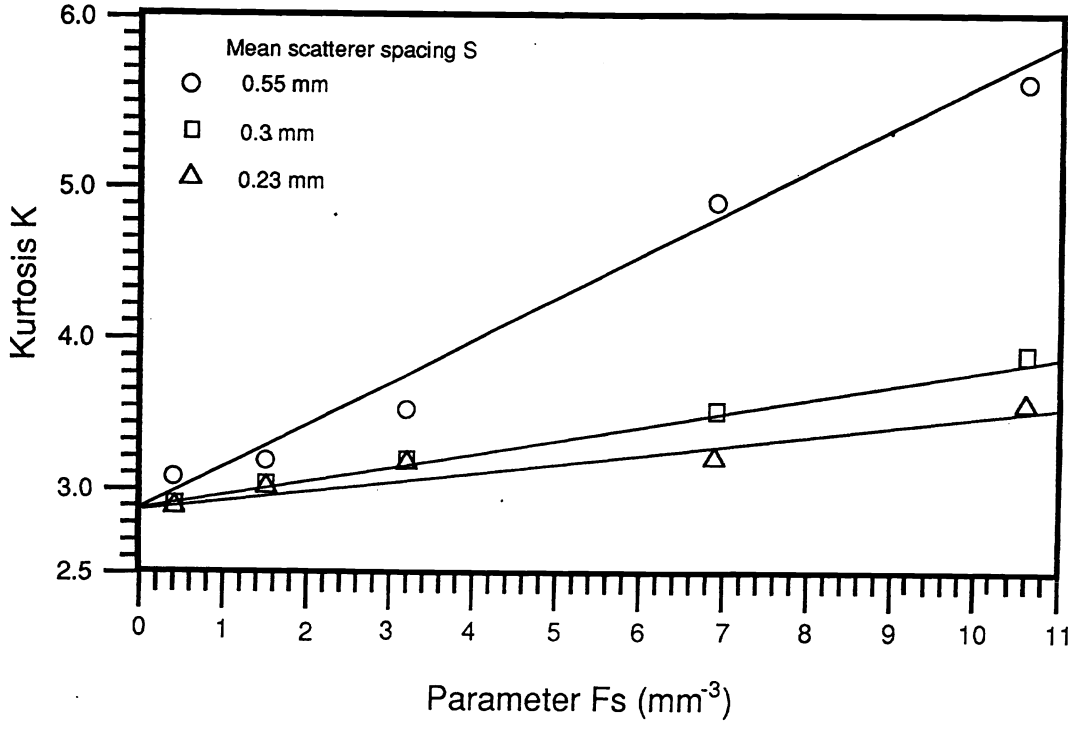

Figure 11 Kurtosis vs resolution cell volume dependent parameter F_s for three different tissue models.

Three different tissue models were interrogated with five different imaging pulses described in table 1. All three models had the same gaussian statistics for random scattering strengths so that $F_m = 3$. They differ in terms of mean scatterer spacing S which was chosen to be 0.55 mm, 0.3 mm and 0.23 mm. The final result for all the three models is summarized in figure 11. Average value of Kurtosis K is plotted against the PSF dependent parameter F_s. Three major points can be noted about the graph.

(1) The data for the three models is shown with different symbols. In all the three cases, Kurtosis deviates from its limiting value of 3 as F_s increases. An increase in F_s implies a decrease in the resolution cell volume, and therefore for a given tissue model a decrease in the number of scatterers within a cell. It is the drop in this number that ultimately accounts for the observed departure from limiting behavior. As F_s approaches zero, the number of scatterers within the resolution cell volume becomes large in the case of all the three tissue models. Kurtosis approaches a value of 3, indicating that RF signal is gaussian distributed. By a least square fit to equation (11) we find this limiting value to be about 2.9.

(2) The theory {equation (11) predicts that the estimate of Kurtosis should increase linearly with parameter F_s, for a given tissue model. This is borne out by the behavior of our data. K increases linearly with F_s for all the three tissue models (Figure 11).

(3) The theory also predicts that the slope of the linear plot depends on the statistical properties of the interrogated random medium. The slope is given by (F_m/SND). Qualitatively, as S increases, SND should decrease and therefore the slope should increase. This is what we observe in figure 11, the slope increases with mean scatterer spacing S. It is assumed that $F_m = 3$ for all the three models. A least square fit was performed to estimate the slope in all three cases. SND was estimated from the slope values and mean scatterer spacing S was calculated from SND. The calculated values of S were found to be 0.48 mm, 0.34 mm and 0.31 mm. Agreement with the original values for the three models is good, considering the fact that simulation process was discrete, with the 3D scattering region split into several discrete microbeams.

5. SUMMARY

A computer model, to simulate backscattered RF signal from a 3D random medium has been described. The model utilizes the radial symmetry of the transducer and is very useful in generating different RF signals in response to the different interrogating pulses. A technique that uses frequency modulated pulses for imaging is outlined, to facilitate variations in the PSF of the imaging system. The objective was to study changes in the RF signal as a function of the PSF of the imaging system as well as the random medium that is under investigation. The RF signal simulation was performed for three different random tissue models. Each model was further interrogated with five different FM pulses. Stochastic signal analysis of the RF signal was performed and the results were compared with theoretical predictions [2].

Guided by the analysis of the RF signal, a method for tissue characterization can be formulated. The central feature of the technique is to "image" the same random medium with different point spread functions. Analogous to "multispectral imaging" in remote sensing, this could be termed as "multi PSF imaging." The multiple data set can then be analyzed to extract structural

parameters of the tissue or the random medium

6. ACKNOWLEDGEMENTS

This project was supported in part by a grant-in-aid award from the American Heart Association, No. 881095.

REFERENCES

1

1. Burckhardt, C.B. "Speckle in ultrasound B-mode scans," IEEE Trans. on Sonics & Ultrasonics, Vol. 25, pp. 1-t, 1978.

2. Sleefe, G.E. and P. Lele, "Tissue characterization based on scatterer number density estimation," IEEE Trans. on UFFC, Vol. 35, No. 6, pp. 749-757, 1988.

3. Osterveld, B.J., Thijssen, J.M., and Verhoel, W.A., "Texture of B-mode echograms" 3-D simulations and experiments of the effects of diffraction and scatterer density," *Ultrasonic Imaging* 7, 142-160, 1985.

4. Rao, N.A.H.K., E.R. Ritenour, R.E. Hendrick, "Frequency Modulated Pulse for Ultrasonic Imaging," SPIE Proceedings on Medical Imaging II, Vol. 914, 67-74, 1988.

5. Rao, N.A.H.K., "Frequency Modulated Pulse for Ultrasonic Imaging in an Attenuating Medium," Proc. 3rd IEEE Symposium on Computer Based Med. Systems, pp. 89-95, 1990.

6. Arditi, M., W. Taylor, F. Foster, and J. Hunt, "An annular array system for high resolution breast echography," Ultrasonic Imaging, Vol 4, pp 1-31, 1982; also see Vol 3, pp 37-61, 1981.

7. Kuc R. and H. Miwa, "A computer model for simulating reflected ultrasound signals," J. Acoust. Soc. Am., Vol. 80, pp 951-54, (1986).

8. Verhoef, W.S., M.J.T.M. Cloostermans and J.M. Thijssen, "The impulse response of a focused source with an arbitrary axisymetric surface velocity distribution," J. Acoust. Soc. Am., Vol. 75, pp 1716-1721, (1984).

9. Kuc, R., "Ultrasonic tissue characterization using Kurtosis," IEEE Trans. Ultrasonics Ferroelec. Freq. Contr., UFFC-33, No. 3, pp 273-279, 1986.

10. Wagner, R.F., M.F. Insana. Brown, D.G., "Statistical properties of radio frequency and envelope-detected signals with applications to medical ultrasound," J. Opt. Soc. Am., Vol. 4, pp. 910-922, 1987.

11. Cardoso, J.F., "3-D Ultrasonic speckle modeling: below the Rayleigh limit," International Symposium on Pattern Recognition and Acoustical Imaging, SPIE Vol.. 768, pp 207-214, 1987.

12. Goodman, J.W., Statistical Optics (J. Wiley, NY 1985).